

Calculation of Optimum Thickness of Active Layer of Oxygen and Air Cathodes of Fuel Cell with Nafion and Platinum

Yu. G. Chirkov^{a,z} and V. I. Rostokin^b

^a*Frumkin Institute of Physical Chemistry and Electrochemistry, Russian Academy of Sciences, Leninskii pr. 31, Moscow, 119991 Russia*

^b*Moscow Institute of Engineering Physics, Kashirskoe sh. 31, Moscow, 117409 Russia*

Received February 15, 2008

Abstract—It is shown that, for the electrodes of fuel cells with solid polymer electrolyte, the dependence of overall current on the active layer thickness contains an extremum. There is an optimum thickness of active layer, at which the overall current reaches its maximum possible value. The nature of this dependence is explained. The character of the distribution of electrochemical process intensity over the width of active layer of cathode with solid polymer electrolyte is analyzed. The optimum thicknesses of active layers of oxygen and air cathodes of fuel cells with Nafion and platinum and the corresponding overall currents and contents of catalyst in the active layer are calculated. In the calculations, the temperature of fuel cell, the pressure in the cathode gas chamber, and the cathodic potential were varied. The optimization of active layer thickness of cathode with solid polymer electrolyte can reduce the platinum consumption, i.e. its amount per 1 kW of power produced in a membrane–electrode block.

Key words: fuel cell with Nafion and platinum; oxygen and air cathodes; computer-aided simulation of current generation in an active layer; optimum thickness of active layer

DOI: 10.1134/S1023193509020098

INTRODUCTION

Fuel cells with solid polymer electrolyte (commonly, Nafion) have the following advantages as the power sources: they exhibit a high power and sufficiently long service life, can operate at low temperatures, are compact, environmentally save, and noiseless. These power sources can be used in the vehicles, under the stationary conditions, in the computers, and in various sensors. The commercialization of these fuel cells is hampered, predominantly, by the use of platinum as the catalyst in them.

Platinum is expensive and its reserves are limited. In 2004, only 202 tons of platinum was mined. At the same time, the amount of platinum required, for example, for replacing all internal-combustion engines in the cars by the electric motors energized from the fuel cells with solid electrolyte is comparable to its world reserves (100 000 tons). In addition, fuel cells containing platinum are required for other types of vehicles and for stationary independent power sources.

There are two lines of attack on this problem. First, the development of catalysts free of platinum, primarily, chalcogenides with transient metals, macrocyclic complexes with transient metals [1], and binary catalysts (alloys of RuX, PdX, etc. types, where X = Co, Ni, Fe, etc.) [2]. Unfortunately, no great success in this field

has been achieved; on the whole, the substitutes are exceeded by platinum both in activity and stability.

Second, the catalytic ability of various alloys of platinum with transient metals, for example, the alloys of Pt_xCo_{1-x}/C type, is investigated. This approach to the problem of platinum was started in [3, 4]. These nanodimensional catalytic systems, which require lower platinum consumption, approach traditional catalysts (platinum applied to highly dispersed carbon material Pt/C) in their catalytic characteristics [5].

In the fuel cells with solid polymer electrolyte, the cathode, where the oxygen reduction proceeds in the acid medium, is the most problematic point. The kinetics of this process is rather slow. At the hydrogen platinum anode, the overpotential is low (< 25 mV), whereas at the cathode, it can be higher than 500 mV for a current density of ~ 1 A/cm². Therefore, the investigators focus their efforts on the search for platinum substitutes for the cathode.

As for the hydrogen-air fuel cell with solid polymer electrolyte, which is the most popular system, significant but not sufficient success has been achieved. At a loading of a membrane–electrode block (MEB) with 0.6–0.8 mg/cm² platinum at a potential of 0.6 V (corresponding to a fuel cell efficiency of 58% at 80°C and the atmosphere pressure), the specific power of MEB was enhanced to 0.7 W/cm² [6]. The main characteristic of power consumption, namely, its amount per 1 kW of

^z Corresponding author: olga.nedelina@gmail.com.

power generated in the MEB, reached 0.85-1.1 g/kW. This result is the evidence for significant progress as compared with the situation in the 1990th. However, to attract the interest of auto-car constructors to the hydrogen-air fuel cells with Nafion and platinum, it is necessary to reduce the platinum consumption by 5 times more [7].

Fuel cells with solid polymer electrolyte are improved by various means. For instance, the trend has been toward a decrease in the thickness of Nafion membrane leading to a decrease in the ohmic limitations, an increase in the potential, and, as a result, an increase in the specific power of fuel cell. In recent ten years, the membranes have become significantly thinner: from 175/125 μm (Nafion 117/115) [8] to 50 μm (Nafion 112) [9]. At present, the membranes 25 μm thick are coming into use [10].

The content of platinum m (mg/cm^2) on the electrodes of fuel cell can be reduced by improving the processes of mass and electric transfer in the active layer of cathode. Thin active layers are desirable. Therefore, the thickness of active layer steadily decreases: from 100 [11] to present 10–15 μm . Important advantage of thin active layers is a smaller content of expensive catalysts of platinum group as compared with thick active layers.

It is easy to show that a specific content of catalyst in the active layer with thickness Δ can be estimated by the following equation:

$$m = g_s(1 - v)\rho_s[g_w/(1 - g_w)]\Delta, \quad (1)$$

Here, g_s is the bulk concentration of substrate (carbon black) grains in the active layer, v is the porosity of substrate grains, ρ_s is the density of carbon material, g_w is the weight content of platinum in the carbon substrate grains. Taking $g_s = 0.6$, $v = 0.5$, $\rho_s = 1.8 \text{ g}/\text{cm}^3$, $\Delta = 10 \mu\text{m}$, we obtain: for $g_w = 20 \text{ wt } \%$, $m = 0.135 \text{ mg}/\text{cm}^2$; for $g_w = 50 \text{ wt } \%$, $m = 0.54 \text{ mg}/\text{cm}^2$. Correspondingly, with a decrease in the active layer thickness, for example, to $\Delta = 4 \mu\text{m}$, m will decrease to 0.054 (for $g_w = 20 \text{ wt } \%$) and 0.216 mg/cm^2 (for $g_w = 50 \text{ wt } \%$).

However, several intricate questions arise. What thickness of cathode active layer, for example, with Nafion and platinum, should be chosen as optimum, taking into account that it depends on many factors:

(1) the conditions of fuel cell operation (the temperature, pressure in the gas chamber of cathode, the cathodic potential);

(2) the parameters characterizing the composition and structure of active layer (average sizes of Nafion and substrate grains; bulk concentrations of these grains and void fraction; a fraction of platinum specific surface area, which is really involved in the electrochemical process);

(3) the peculiarities of kinetics of oxygen reduction on platinum in the acid medium.

Certainly, the active layer thickness can be chosen empirically, but this way is difficult and long. It is much

easier to use the computer simulation of cathode active layer structure and the processes of current generation in it, to follow the procedures of calculating the overall characteristics of cathodes of fuel cells with solid polymer electrolyte, which were developed in [12–15].

Here, we will estimate the optimum thickness of active layer of cathode of fuel cell with Nafion and platinum under various conditions of cell operation with the aid of computer simulation.

SELECTION OF PARAMETERS OF ACTIVE LAYER OF CATHODE WITH NAFION AND PLATINUM

Prior to calculating the optimum thicknesses of active layer of cathode with Nafion and platinum, it is necessary to choose the parameters characterizing an active layer (these parameters are listed at the end of the paper).

The active layer parameters can be clearly divided into several groups characterizing:

- (1) external conditions of fuel cell operation;
- (2) the electrochemical process of oxygen reduction on platinum;
- (3) the parameters of active layer structure;
- (4) true and effective coefficients describing mass and electric transfer.

External parameters. These are, as was noted above, the operation temperature of fuel cell t , the pressure in the cathode gas chamber p^* , the cathode active layer thickness Δ (its optimum value Δ^* will be determined).

Parameters of electrochemical kinetics of oxygen reduction on platinum. It is commonly assumed that in the oxygen reduction on platinum in the acid media and, consequently, in the active layer of cathode with Nafion, two slopes of Tafel curve are observed: 60 mV (in the range of high potentials) and 120 mV (in the range of low potentials). However, in [5], this generally accepted opinion, which was supported by many results obtained both in the model experiments (on a rotating disk electrode, etc.) and directly in the H_2 - O_2 MEB (for example, [16–19]), was questioned and considered as an artifact.

Without going into details of scientific discussion raised in [5], we assume that the Tafel plot has two slopes. In the case that the polarization curves of catalyst contain several segments with different slopes, the overall currents and other characteristics of active layers of cathodes with Nafion and platinum should be calculated as it was shown in [20].

50% Pt/C (TKK) was chosen as the catalyst. In addition, for the sake of definiteness, we assume that the steady-state cathodic potential $E_{st} = 1.05 \text{ V}$, an inflection in the Tafel curve is observed at the potential $E^* = 0.825 \text{ V}$, and the reduced slopes of Tafel curves are $b_1 = (6/2.3) \times 10^{-2} = 2.6 \times 10^{-2} \text{ V}$ and $b_2 = (12/2.3) \times 10^{-2} =$

5.2×10^{-2} V in the ranges of high and low potentials, respectively.

According to [21], at a temperature of 50°C, the exchange current i_0 is 10^{-8} A/cm². Using the equation for the temperature dependence of exchange current (the oxygen reduction on platinum), which was proposed in [22], we obtain $i_0 = 2.27 \times 10^{-8}$ A/cm² at the temperature $t = 60^\circ\text{C}$, $i_0 = 1.01 \times 10^{-7}$ A/cm² at $t = 80^\circ\text{C}$, and $i_0 = 2.80 \times 10^{-7}$ A/cm² at $t = 95^\circ\text{C}$.

Parameters of optimum structure of active layer.

Assume, as it was proposed in [12–14], that the structure of active layer of fuel cell cathode with Nafion and platinum can be described using the model of equidimensional grains (the grains of Nafion and substrate). The Nafion grains are the agglomerates of molecules of solid polymer electrolyte (Nafion), and the substrate grains are the agglomerates of substrate (carbon black) particles with platinum nanoparticles on their surface.

Assume that the active layer structure is optimum. This means that the void fraction in the active layer is zero $g_0 = 0$ (the desirability of this condition was explained in [14]), and the bulk concentrations of Nafion grains g_e and substrate grains g_s are roughly equal. More exactly, as was shown by the computer-aided calculations, the overall current reaches the maximum value at $g_e = 0.475$. Then, obviously (at $g_0 = 0$), $g_s = 0.525$. In addition, assume that the pore size in the substrate grains $d_s = 30$ nm, and the porosity of substrate grains $v = 0.5$.

The equation for the overall characteristics of cathode active layer involves four parameters [20]: the effective diffusion coefficient of oxygen D^* , the effective conductivity of protons k^* , the solubility of oxygen in Nafion c_o , and the characteristic bulk current density i^* (here, the dimensionality of i^* is A/cm³). The bulk current density is determined by the following equation:

$$i^* = i_0 \eta g_s S, \quad (2)$$

where i_0 is the exchange current, g_s is the bulk concentration of substrate grains, and S is the specific surface area of platinum in a unit volume, which is completely filled with substrate grains. Thus, the product $g_s S$ is the specific surface area of platinum in a unit volume of active layer. The peculiarity of the electrodes with solid polymer electrolyte is that only a fraction of the catalyst, which is present in the active layer, can be involved in the process of current generation. The active catalyst fraction is designated as η . Then, the product $\eta g_s S$ is the specific surface area of platinum in the active layer, which is really involved in the current generation.

Now, we define the surface area S , which is involved in the theoretical equations. Commonly, not this value, which has dimensionality $\text{cm}^2/\text{cm}^3 = \text{cm}^{-1}$, but a specific surface area of platinum per unit platinum weight S^* , which has dimensionality $\text{m}^2/\text{g Pt}$, is determined experimentally. Therefore, it is necessary to relate S to S^* .

By definition, the content of platinum in the substrate grains

$$g_w = V_p \rho_p / (V_p \rho_p + V_s \rho_s), \quad (3)$$

where V_p and V_s are the fractions of platinum and carbon black volumes in a unit volume completely filled with substrate grains, respectively; ρ_p and ρ_s are the densities of platinum and carbon black. Obviously, for a unit volume completely filled with the substrate,

$$V_p + V_s + v = 1, \quad (4)$$

where v is the void fraction of substrate grains. Eliminating V_s from (3) and (4), we determine V_p

$$V_p = (1 - v) / [1 + (\rho_p / \rho_s) [(1 - g_w) / g_w]]. \quad (5)$$

Obviously,

$$S = \rho_p V_p S^*, \quad (6)$$

Then, taking into account (5), we finally obtain

$$S = \rho_p S^* (1 - v) / [1 + (\rho_p / \rho_s) [(1 - g_w) / g_w]]. \quad (7)$$

In the calculations, we take $\rho_p = 21.5$ g/cm³, $\rho_s = 1.8$ g/cm³, $g_w = 60$ wt %, $S^* = 86$ m²/g Pt [7]. Thus, we obtain that the specific surface area of platinum in the active layer of cathode with Nafion is $S = 1.03 \times 10^6$ cm⁻¹.

A fraction of surface area S , which is involved in the electrochemical process (designated as η), varies from $\eta = 60$ –70 [23] to 75–98% [24, 25]. We take $\eta = 90\%$. Using equation (2), we obtain that, in the high potential range, the characteristic bulk current densities i^* (A/cm³) are 1.10×10^{-2} , 4.92×10^{-2} , and 1.36×10^{-1} at the temperatures of 60, 80, and 95°C, respectively.

Parameters determining mass and electric transfer. As was shown by the computer-aided calculations (the model of equidimensional grains [14]), in the active layer with Nafion, provided that $g_0 = 0$ (zero void fraction) and $g_e = 0.475$, the effective diffusion coefficient of oxygen $D^* = 5.49 \times 10^{-4}$ cm²/s and the effective proton conductivity $k^* = 8.37 \times 10^{-3}$ Ω^{-1} cm⁻¹ (at the optimum conductivity of Nafion $k = 0.1$ Ω^{-1} cm⁻¹).

The solubility of oxygen in Nafion c_o depends on the pressure according to the Henry law. Assume that at $p^* = 101$ kPa, $c_o = 5 \times 10^{-6}$ g-mol/cm³ [26]. Then, at $p^* = 150$ kPa, which was chosen for the calculations, the solubility $c_o = 7.43 \times 10^{-6}$ g-mol/cm³.

Then, we calculate the overall currents for oxygen and air cathodes. Formally, they differ in the boundary conditions for supersaturation of Nafion with gas at the active layer/gas-diffusion layer (GDL) interface: $y = \Delta c / c_o = 1$ for the oxygen cathode (at the inner surface of active layer) and $y = \Delta c / c_o = 0.21$ for the air cathode.

CALCULATION OF OPTIMUM THICKNESS OF ACTIVE LAYER OF CATHODE WITH NAFION AND PLATINUM

In the main part of the study, we analyze the effect of active layer thickness on the overall current of the

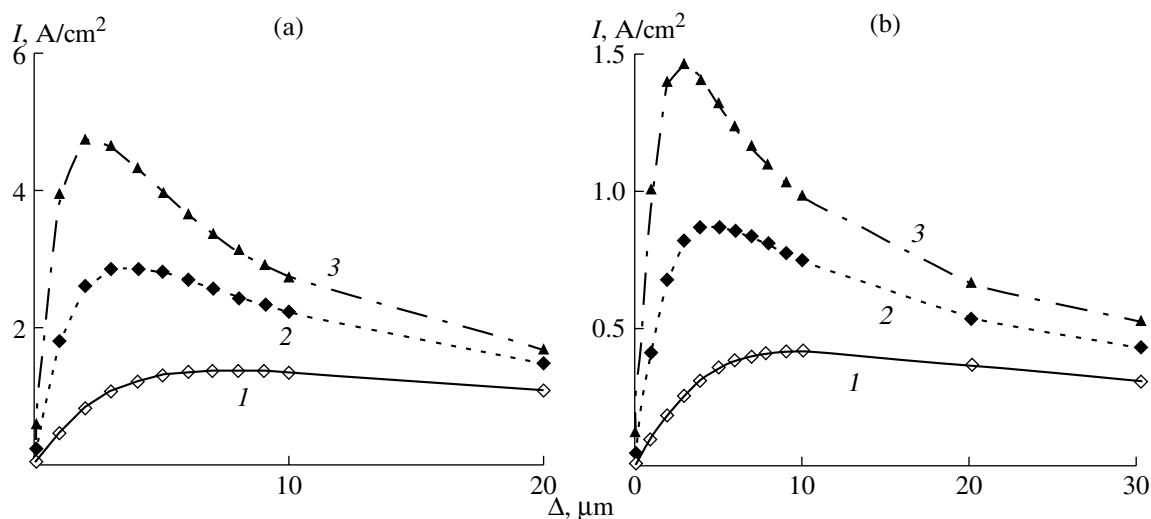


Fig. 1. Dependences of overall current, which is generated in the active layer of (a) oxygen and (b) air cathodes of fuel cell with Nafion and platinum, on the active layer thickness at $t^{\circ}\text{C}$: (1) 60, (2) 80, and (3) 95; $E_0 = 0.6\text{ V}$; $p^* = 150\text{ kPa}$.

cathode with Nafion and platinum and determine the optimum thickness. In the electrodes with solid polymer electrolyte (Nafion), protons move along a percolation cluster consisting of chains of solid polymer electrolyte grains connected with each other (agglomerates of Nafion molecules). Gas is delivered to the active layer, predominantly, by another percolation cluster consisting of chains of substrate (carbon black) grains connected with each other. At the optimum moistening of active layer, small (tens of nm in size) pores of these grains remain free of electrolyte. In these pores, the Knudsen diffusion of gases takes place.

Thus, in the active layer of cathode with Nafion, not only the ohmic limitations (the motion of protons from the front surface of active layer, from its boundary with the Nafion membrane), but also the intradiffusion limitations (the motion of gas molecules from the inner surface of active layer, from the GDL) should be taken into consideration. As a result, with gradually increasing active layer thickness Δ , initially, the overall current increases, because the entire active layer becomes equally accessible for the delivery of both oxygen molecules and protons. However, the situation of equal access gradually vanishes, and at a certain active layer thickness ($\Delta = \Delta^*$), the overall current I reaches its optimum value. Then, it decreases to zero, because the sources of protons (the front surface of active layer) and gas (the inner surface of active layer) progressively remove from each other, and the ohmic and intradiffusion limitations indefinitely increase.

The latter conclusion is not obvious; therefore, we will support it by calculating the dependence of overall current on the thickness of active layer of cathode with Nafion and platinum. The parameters, which are used for the calculations, are discussed above and listed at the end of the paper. The overall currents will be calculated by the equations presented in [20].

Figure 1 gives the calculated dependences of overall currents I , which are generated in the active layer of (a) oxygen and (b) air cathodes of fuel cell with Nafion and platinum, on the active layer thickness Δ at the cathode potential $E_0 = 0.6\text{ V}$. The temperature of cathode was varied leading to the variations of the characteristic bulk current density on the cathode. Curves 1–3 (Fig. 1) correspond to the temperatures t , $^{\circ}\text{C}$: (1) 60, (2) 80, and (3) 95. The corresponding characteristic bulk current densities i^* (A/cm³) are 1.10×10^{-2} , 4.92×10^{-2} , and 1.36×10^{-1} .

Figure 1, firstly, supports the presence of extremum in the plots of I vs. Δ for the cathodes with solid polymer electrolyte. Secondly, it is seen that the maximum in the I vs. Δ curves becomes sharper and shifts to smaller optimum thickness Δ^* (the thickness, at which the overall current reaches its maximum I^*) with increasing temperature. At $t = 60^{\circ}\text{C}$, the maximum is blurred. We can roughly consider that, on Fig. 1, near the oxygen cathode, $\Delta^* = 8\ \mu\text{m}$ and the maximum current $I^* = 1.36\text{ A/cm}^2$, and, near the air cathode, $\Delta^* = 10\ \mu\text{m}$ and the maximum current $I^* = 0.42\text{ A/cm}^2$.

Similar parameters for $t = 80^{\circ}\text{C}$ are $\Delta^* = 4\ \mu\text{m}$, $I^* = 2.87\text{ A/cm}^2$ (oxygen cathode, Fig. 1a) and $\Delta^* = 5\ \mu\text{m}$, $I^* = 0.88\text{ A/cm}^2$ (air cathode, Fig. 1b). At $t = 95^{\circ}\text{C}$: $\Delta^* = 2\ \mu\text{m}$, $I^* = 4.76\text{ A/cm}^2$ (oxygen cathode, Fig. 1a) and $\Delta^* = 3\ \mu\text{m}$, $I^* = 1.47\text{ A/cm}^2$ (air cathode, Fig. 1b). It is seen that, at the elevated temperatures, the optimum thickness of cathode active layer should be chosen accurately. For instance, for oxygen cathode at $t = 95^{\circ}\text{C}$ (Fig. 1a), for an active layer with thickness $\Delta = 1\ \mu\text{m}$, the overall current $I = 3.99\text{ A/cm}^2$; for a layer with thickness $\Delta = 4\ \mu\text{m}$, the overall current $I = 4.33\text{ A/cm}^2$. These currents (3.99 and 4.33 A/cm²) considerably differ from the optimum overall current $I^* = 4.76\text{ A/cm}^2$, which is reached at the optimum thickness $\Delta^* = 2\ \mu\text{m}$.

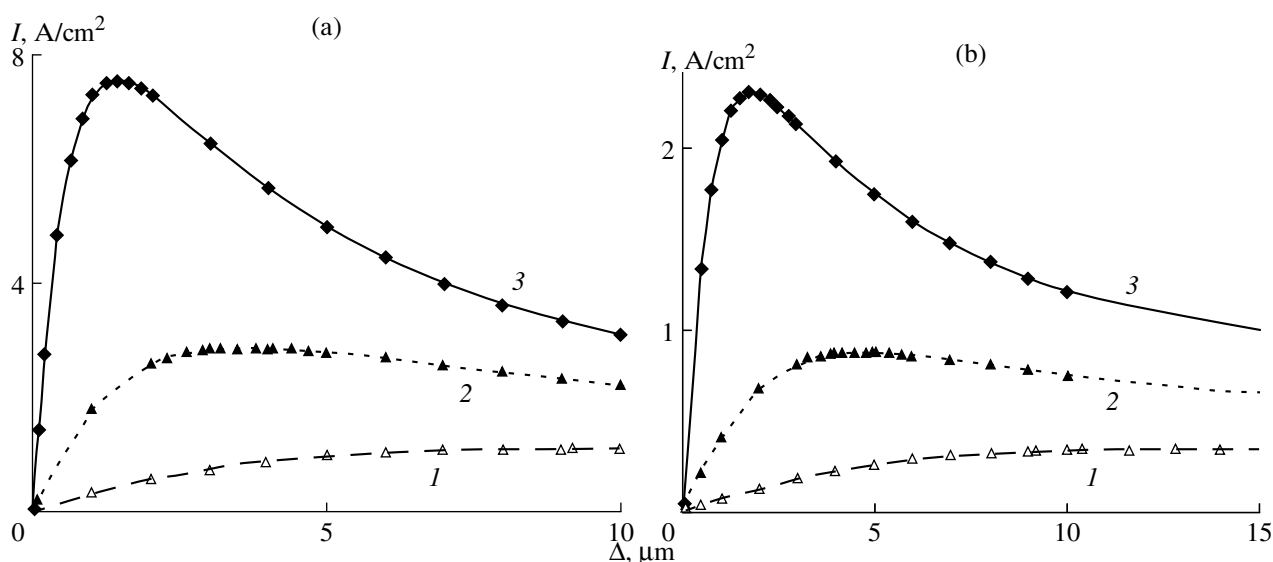


Fig. 2. Dependences of overall current, which is generated in the active layer of (a) oxygen and (b) air cathodes of fuel cell with Nafion and platinum, on the active layer thickness. E_0 , V: (1) 0.7, (2) 0.6, and (3) 0.5; $t = 80^\circ\text{C}$; $p^* = 150$ kPa.

At a temperature $t = 95^\circ\text{C}$ (Fig. 1b), the maximum current on the air cathode $I^* = 1.468$ A/cm² is reached at the active layer thickness $\Delta^* = 3$ μm. It should be noted that the optimum content of platinum in the active layer m^* (it can be calculated by equation (1), substituting Δ^* for Δ) varies with increasing temperature. In the curves 1–3 (Fig. 1), the temperatures t , °C: (1) 60, (2) 80, and (3) 95 correspond to the values of m^* , mg/cm²: 0.38, 0.19, 0.095 (oxygen cathode) and 0.47, 0.24, 0.14 (air cathode).

Now, we analyze the variation of Δ^* and I^* with the cathode potential E_0 . Figure 2 gives the plots of the overall currents I , which are generated in the active layer of (a) oxygen and (b) air cathodes of fuel cell with Nafion and platinum, on the active layer thickness Δ at $t = 80^\circ\text{C}$. The cathode potential was varied. The curves 1–3 (Fig. 2) correspond to the potentials E_0 , V: (1) 0.7, (2) 0.6, and (3) 0.5.

The optimum overall current I^* steeply increases and the optimum active layer thickness Δ^* and, correspondingly, the optimum content of platinum in the active layer m^* decrease with decreasing potential. The precise data are as follows. For oxygen cathode: $\Delta^* = 9.2$ μm, $I^* = 1.1$ A/cm², and $m^* = 0.43$ mg/cm² (Fig. 2a, curve 1); $\Delta^* = 3.8$ μm, $I^* = 2.87$ A/cm², and $m^* = 0.18$ mg/cm² (Fig. 2a, curve 2); $\Delta^* = 1.4$ μm, $I^* = 7.51$ A/cm², and $m^* = 0.07$ mg/cm² (Fig. 2a, curve 3). For air cathode: $\Delta^* = 12.8$ μm, $I^* = 0.34$ A/cm², and $m^* = 0.60$ mg/cm² (Fig. 2b, curve 1); $\Delta^* = 4.8$ μm, $I^* = 0.88$ A/cm², and $m^* = 0.23$ mg/cm² (Fig. 2b, curve 2); $\Delta^* = 1.75$ μm, $I^* = 2.31$ A/cm², and $m^* = 0.08$ mg/cm² (Fig. 2b, curve 3).

To determine the reason for an extremum in the dependence of overall current on the active layer thickness in the cathodes with solid polymer electrolyte, the distributions of basic current-determining values,

namely, potential and the supersaturation of Nafion with oxygen, over the active layer should be calculated at various active layer thicknesses.

Figure 3 shows the distribution of (a) potential and (b) the supersaturation of Nafion with oxygen across the reduced width (the y/Δ coordinate, it is measured from the Nafion membrane/active layer interface) of active layer of oxygen cathode with Nafion and platinum. The calculations are performed for the following conditions: the fuel cell temperature $t = 80^\circ\text{C}$, the pressure in the gas chamber $p^* = 150$ kPa, and a cathodic potential E_0 of 0.6 V. The curves on Fig. 3a differ in the active layer thickness Δ , μm: (1) 1, (2) 3.8, (here, $\Delta = \Delta^*$, and the overall current reaches its maximum value), (3) 10, (4) 50, and (5) 90.

Clearly, in thin active layers (Fig. 3, curves 1), ohmic and intradiffusion losses are small (the condition of equal access is valid: the entire surface area of platinum, which is accessible for electrocatalysis, generates the current under the kinetic control). Therefore, the deviations of potential near the inner surface of active layer $E(y = \Delta) = E_s$ from the cathodic potential E_0 (the front surface of active layer) and of Nafion supersaturation with oxygen near the front surface c/c_0 ($y = 0$) ($y = 0$) from that near the inner surface ($y = \Delta$), where $c/c_0 = 1$, are insignificant. However, with increasing thickness of active layer, the ohmic and diffusion limitations become more and more considerable. The potential near the inner surface E_s increases and tends to the steady state cathodic potential $E_{st} = 1.05$ V. The supersaturation of Nafion with oxygen on the front surface decays to zero and, as it is seen from Fig. 3b, the range of current generation is gradually localized near the inner surface of cathode active layer.

All aforesaid about the active layer of oxygen cathode is qualitatively true for the active layer of air cathode

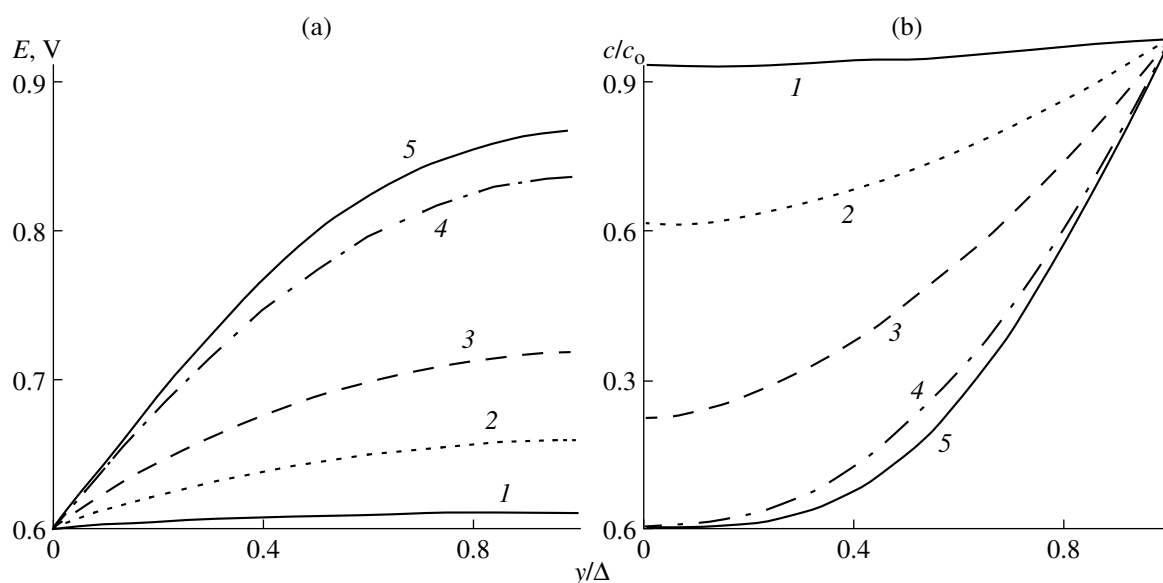


Fig. 3. Distribution of (a) potential and (b) supersaturation of Nafion with oxygen across the reduced width of active layer of oxygen cathode of fuel cell with Nafion and platinum. Δ , μm : (1) 1, (2) 3.8, (here, $\Delta = \Delta^*$), (3) 10, (4) 50, and (5) 90; $t = 80^\circ\text{C}$, $p^* = 150$ kPa, $E_0 = 0.6$ V.

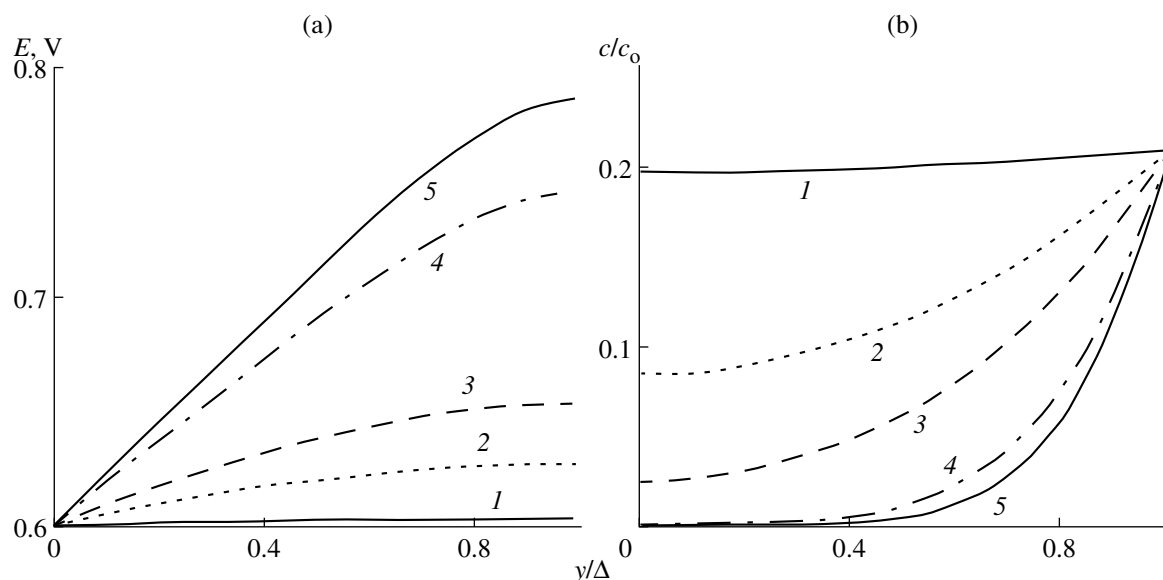


Fig. 4. Distribution of (a) potential and (b) supersaturation of Nafion with oxygen across the reduced width of active layer of air cathode of fuel cell with Nafion and platinum. Δ , μm : (1) 1, (2) 4.8, (here, $\Delta = \Delta^*$), (3) 10, (4) 50, and (5) 90; $t = 80^\circ\text{C}$, $p^* = 150$ kPa, $E_0 = 0.6$ V.

ode. Figure 4 gives the distribution of (a) potential and (b) the supersaturation of Nafion with oxygen over the reduced width of active layer of air cathode of fuel cell with Nafion and platinum. The calculations are performed for the following conditions: the fuel cell temperature $t = 80^\circ\text{C}$, the pressure in the gas chamber $p^* = 150$ kPa, and the cathodic potential E_0 of 0.6 V. The curves on Fig. 4a differ in the active layer thickness Δ ,

μm : (1) 1, (2) 4.8, (here, $\Delta = \Delta^*$, and the overall current reaches its maximum value), (3) 10, (4) 50, and (5) 90.

The concept that, at a considerable increase in the active layer thickness, the zone of current generation is concentrated near the inner surface of active layer is supported also by the data presented on Fig. 5. Figure 5 shows the calculated distributions of the bulk current density, which is generated in the active layer of cathode, over the reduced width (y/Δ) of active layer of (a)

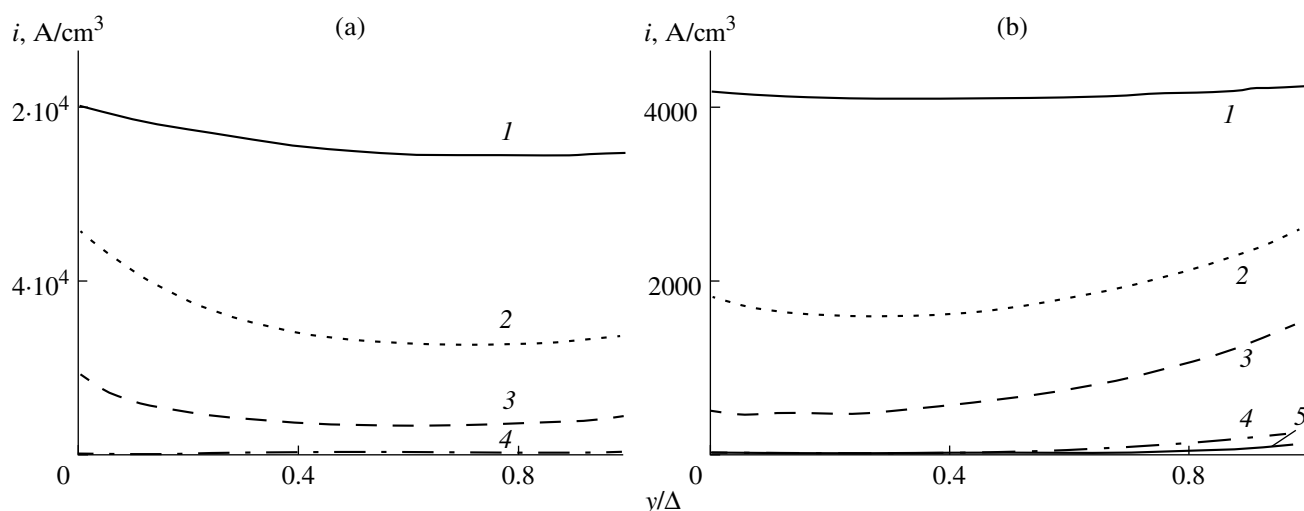


Fig. 5. Distribution of current density, which is generated in the active layer, across the reduced width of active layer of (a) oxygen and (b) air cathodes of fuel cell with Nafion and platinum. Δ , μm : (1) 1, (2) 3.8, (Fig. 5a, here $\Delta = \Delta^*$) and 4.8 (Fig. 5b, here $\Delta = \Delta^*$), (3) 10, (4) 50, and (5) 90; $t = 80^\circ\text{C}$, $p^* = 150\text{ kPa}$, and $E_0 = 0.6\text{ V}$.

oxygen and (b) air cathodes of fuel cell with Nafion and platinum. The curves on Fig. 5 differ in the active layer thickness Δ , μm : (1) 1, (2) 3.8, (Fig. 5a, here $\Delta = \Delta^*$) and 4.8 (Fig. 5b, here $\Delta = \Delta^*$), (3) 10, (4) 50, and (5) 90. The fuel cell temperature $t = 80^\circ\text{C}$, the pressure in the gas chamber $p^* = 150\text{ kPa}$, and the cathodic potential $E_0 = 0.6\text{ V}$.

On the oxygen cathode (Fig. 5a), the bulk current density near the front surface of active layer is higher than that near the inner surface. Probably, this is due to the fact that the intradiffusion limitations in the oxygen cathode should be less significant as compared with the air cathode: in the oxygen cathode, on the inner surface of active layer, the supersaturation of Nafion with oxygen is significant ($c/c_0 = 1$). A different situation is observed on the air cathode (Fig. 5b). Here, the intradiffusion limitations are more rigid, because, as compared with the oxygen cathode, the supersaturation of Nafion with oxygen on the inner surface of active layer on the air cathode is lower: $c/c_0 = 0.21$. Therefore, in the air cathode, the bulk current density appears to be higher not near the front surface of active layer, but near its inner surface.

It should be noted that, near the cathodes with optimum thickness (Figs. 5a and 5b, curves 2), the bulk current densities are high: about 10^4 A/cm^2 near the oxygen cathode and $2 \times 10^3\text{ A/cm}^2$ near the air cathode. However, with increasing thickness of active layers, the current densities decrease, and the current generation gradually localizes near the inner surface of active layer (this is most pronounced on Fig. 5b).

Thorough analysis of the data presented on Figs. 3–5 suggests that, in the cathodes with Nafion and platinum, the intradiffusion limitations are more severe than the ohmic limitations, since the variation in the supersaturation of Nafion with oxygen across the active layer width c/c_0 dominates over the variation in the overvolt-

age E . Therefore, it is reasonable to raise the overall current by increasing oxygen pressure p^* in the gas chamber, because the solubility of oxygen in Nafion c_0 increases linearly with the pressure (according with the Henry law).

Figure 6 gives the calculated dependences of overall current, which is generated in the active layer of (a) oxygen and (b) air cathodes of fuel cell with Nafion and platinum at the temperature $t = 80^\circ\text{C}$ and cathodic potential $E_0 = 0.6\text{ V}$, on the active layer thickness. The gas pressure p^* in the gas chamber was varied: (1) 101, (2) 303, and (3) 505 kPa.

Optimum overall currents, thicknesses of active layer, and contents of platinum in it for oxygen cathode (Fig. 6a) are as follows. At $p^* = 101\text{ kPa}$: $I^* = 2.64\text{ A/cm}^2$, $\Delta^* = 3.1\text{ }\mu\text{m}$, and $m^* = 0.15\text{ mg/cm}^2$; at $p^* = 303\text{ kPa}$: $I^* = 3.23\text{ A/cm}^2$, $\Delta^* = 4.8\text{ }\mu\text{m}$, and $m^* = 0.23\text{ mg/cm}^2$; at $p^* = 505\text{ kPa}$: $I^* = 3.45\text{ A/cm}^2$, $\Delta^* = 5.5\text{ }\mu\text{m}$, and $m^* = 0.26\text{ mg/cm}^2$. The parameters of air cathode (Fig. 6b) are lower. At $p^* = 101\text{ kPa}$: $I^* = 0.775\text{ A/cm}^2$, $\Delta^* = 4.1\text{ }\mu\text{m}$, and $m^* = 0.19\text{ mg/cm}^2$; at $p^* = 303\text{ kPa}$: $I^* = 1.08\text{ A/cm}^2$, $\Delta^* = 6.0\text{ }\mu\text{m}$, and $m^* = 0.28\text{ mg/cm}^2$; at $p^* = 505\text{ kPa}$: $I^* = 1.22\text{ A/cm}^2$, $\Delta^* = 7.0\text{ }\mu\text{m}$, and $m^* = 0.33\text{ mg/cm}^2$.

Figure 6 shows that, with increasing pressure in the gas chamber, the largest gain in the overall current is obtained, when we pass from the atmospheric pressure ($p^* = 101\text{ kPa}$) to a higher pressure (from curve 1 to curve 2, Fig. 6). Further increase of pressure in the gas chamber slightly changes the overall current (from curve 2 to curve 3, Fig. 6). That is why, in practice, commonly, the pressure in the gas chamber is slightly increased. For similar reason, to calculate the curves presented on Figs. 1–5, a pressure $p^* = 150\text{ kPa}$ rather than $p^* = 101\text{ kPa}$ (atmospheric pressure) was taken.

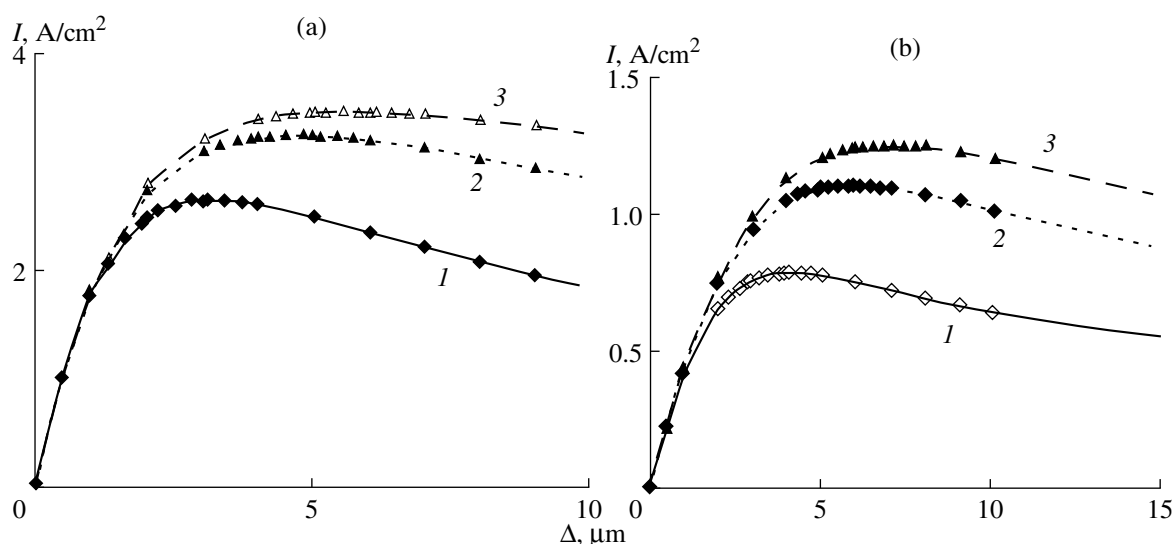


Fig. 6. Dependences of overall current, which is generated in the active layer of (a) oxygen and (b) air cathodes of fuel cell with Nafion and platinum, on the active layer thickness; p^* , kPa: (1) 101, (2) 303, and (3) 505; $t = 80^\circ\text{C}$; and $I - 101$, $2 - 303$, $3 - 505$; $t = 80^\circ\text{C}$, $E_0 = 0.6\text{ V}$.

In conclusion it should be said that, as was mentioned at the beginning of the paper, for the hydrogen–air MEB, at a potential of 0.6 V, pressure $p^* = 101\text{ kPa}$, and $t = 80^\circ\text{C}$, the consumption of platinum per 1 kW of power generated in the MEB reached a record value of 0.85–1.1 g/kW [6]. This data should be compared with the curve 1, Fig. 6b. For this curve, using the above-listed parameters of the curve, we obtain: $m^*/I^*V = 0.19/(0.775 \times 0.6) = 0.41\text{ g/kW}$. This value appeared to be more than two times smaller than the experimental one [6]. The reason for the discrepancy can be explained by two facts. Firstly, the overall characteristics were calculated for the cathodes with highly active catalytic mass: $g_w = 60\text{ wt } \%$, $S^* = 86\text{ m}^2/\text{g Pt}$, and $\eta = 90\%$. Therefore, the calculated overall current appeared to be so high ($I^* = 0.775\text{ A/cm}^2$). Secondly, the restrictions associated with the delivery of oxygen to the active layer of cathode and the removal of water and heat, the ohmic losses in the Nafion membrane, and the overvoltage of anode were ignored in the calculations. All this also will lead to a significant decrease in the overall current. Therefore, a current of 0.41 g/W should be considered as the underneath estimate.

CONCLUSIONS

In contrast to porous hydrophobized electrodes, where the overall current monotonically increases with increasing thickness of active layer and, finally, reaches a maximum value, in the porous electrodes with solid polymer electrolyte, the dependence of overall current on the active layer thickness has an extremum. A certain active layer thickness, at which the overall current reaches its maximum value, should be considered as optimum. Then, the current starts to decrease with increasing thickness. This fact should be taken into

account for optimizing overall characteristics of fuel cells with solid polymer electrolyte.

In the work, the dependences of overall current on the active layer thickness are calculated for oxygen and air cathodes of fuel cells with Nafion and platinum. The temperature, at which the fuel cell operates, the pressure in the gas chamber of cathode, and the cathodic potential were varied. The optimum thicknesses of active layer of cathodes are determined. The values of overall current and the content of catalyst in the active layer corresponding to the optimum thickness are estimated.

LIST OF PARAMETERS CHARACTERIZING AN ACTIVE LAYER OF CATHODE OF FUEL CELL WITH NAFION AND PLATINUM AND THEIR MAGNITUDES TAKEN FOR THE CALCULATIONS

External parameters

- $t = 60, 80, \text{ and } 95^\circ\text{C}$ – temperatures of fuel cell
- $p^* = 150\text{ kPa}$ – pressure in the gas chamber of cathode
- Δ – active layer thickness
- Δ^* – optimum thickness of active layer (will be calculated)

Parameters of electrochemical kinetics of oxygen reduction on platinum

- $E_{\text{st}} = 1.05\text{ V}$ – steady-state potential of cathode
- $E^* = 0.825\text{ V}$ – potential of inflection in the polarization curve

$b_1 = 2.6 \times 10^{-2} \text{ V}$ – slope of polarization curve in the range of high potentials

$b_2 = 5.2 \times 10^{-2} \text{ V}$ – slope of polarization curve in the range of low potentials

$n = 4$ – number of electrons involved in the electrochemical process

$F = 9.6 \times 10^4 \text{ C/mol}$ – the Faraday number

$i_o = 10^{-8} \text{ A/cm}^2$ – exchange current in the range of high potentials at $t = 50^\circ\text{C}$

i^* , A/cm^3 : 1.10×10^{-2} , 4.92×10^{-2} , and 1.36×10^{-1} – the characteristic bulk current densities at $t = 60$, 80 , and 95°C , respectively

Parameters of optimum structure of active layer

$g_e = 0.475$ – bulk concentration of Nafion grains

$g_s = 0.525$ – bulk concentration of substrate grains

$g_o = 0$ – bulk concentration of void grains

$g_w = 60 \text{ wt } \%$ – content of platinum in the substrate grains

$d_s = 30 \text{ nm}$ – average diameter of pores in the substrate grains

$S^* = 86 \text{ m}^2/\text{g Pt}$ – specific surface area of catalyst (platinum) per its unit weight

$S = 1.03 \times 10^6 \text{ cm}^{-1}$ – specific surface area of catalyst (platinum) at $S^* = 86 \text{ m}^2/\text{g Pt}$

$\eta = 90\%$ – a fraction of active surface area of catalyst

$v = 0.5$ – porosity of substrate grains

$\rho_p = 21.5 \text{ g/cm}^3$ – density of catalyst (platinum)

$\rho_s = 1.8 \text{ g/cm}^3$ – density of substrate (carbon black)

Parameters determining the mass and electric transfer processes

$D_{kn} = 4 \times 10^{-3} \text{ cm}^2/\text{s}$ – coefficient of Knudsen diffusion of gas in the pores of substrate grains

$D^* = 5.49 \times 10^{-4} \text{ cm}^2/\text{s}$ – effective diffusion coefficient of oxygen in the active layer

$c_o = 5 \times 10^{-6} \text{ g-mol/cm}^3$ – solubility of oxygen in Nafion at $p^* = 101 \text{ kPa}$

$k = 1 \times 10^{-1} \Omega^{-1} \text{ cm}^{-1}$ – conductivity of optimally moistened Nafion

$k^* = 8.37 \times 10^{-3} \Omega^{-1} \text{ cm}^{-1}$ – effective conductivity of optimally moistened Nafion

REFERENCES

- Zhang, L., Zhang, J., Wilkinson, D., and Wang, H., *J. Power Sources*, 2006, vol. 156, p. 171.
- He, T., Kreidler, E., Xiong, L., Luo, J., and Zhong, C., *J. Electrochem. Soc.*, 2006, vol. 153, p. A1637.
- Mukerjee, S. and Srinivasan, S., *J. Electroanal. Chem.*, 1993, vol. 357, p. 201.
- Mukerjee, S., Srinivasan, S., Soriaga, M.P., and McBreen, J., *J. Electrochem. Soc.*, 1995, vol. 142, p. 1409.
- Neyerlin, K.C., Gu, W., Jorne, J., and Gasteiger, H.A., *J. Electrochem. Soc.*, 2006, vol. 153, p. A1955.
- Wheeler, D.J., Yi, J.S., Fredley, R., Yang, D., Patterson, T., and VanDine, L.: *J. New Mater. Electrochem. Syst.*, 2001, vol. 4, p. 233.
- Gasteiger, H.A., Kocha, S.S., Sompalli, B., and Wagner, F.T., *Appl. Catal. B*, 2005, vol. 56, p. 9.
- Wilkinson, D.P and Steck, A.E, *Proc. 2nd Int. Symposium on New Materials for Fuel Cell and Modern Battery Systems*, Savadogo, O. and Roberge, P.R., Eds., Montreal: Ecole Polytechnique de Montreal, 1997, p. 27.
- Wilkinson, D.P. and St.-Pierre, J., in *Handbook of Fuel Cells - Fundamentals, Technology and Applications*, Vielstich, W., Lamm, A., and Gasteiger, H., Eds., Chichester (UK): Wiley, 2003, vol. 3, ch. 47, p. 611.
- Gasteiger, H.A., Panels, J.E., and Yan, S.G., *J. Power Sources*, 2004, vol. 127, p. 162.
- Costamagna, P. and Srinivasan, S., *J. Power Sources*, 2001, vol. 102, p. 253.
- Chirkov, Yu.G. and Rostokin, V.I., *Elektrokhimiya*, 2004, vol. 40, p. 1036 [*Russ. J. Electrochem. (Engl. Transl.)*, vol. 40, p. 898].
- Chirkov, Yu.G. and Rostokin, V.I., *Elektrokhimiya*, 2005, vol. 41, p. 1109 [*Russ. J. Electrochem. (Engl. Transl.)*, vol. 41, p. 985].
- Chirkov, Yu.G. and Rostokin, V.I., *Elektrokhimiya*, 2006, vol. 42, p. 799 [*Russ. J. Electrochem. (Engl. Transl.)*, vol. 42, p. 715].
- Chirkov, Yu.G. and Rostokin, V.I., *Elektrokhimiya*, 2007, vol. 43, p. 827 [*Russ. J. Electrochem. (Engl. Transl.)*, vol. 43, p. 787].
- Damjanovic, A., Genshaw, M.A., and Bockris, J.O.'M., *J. Phys. Chem.*, 1966, vol. 45, p. 4057.
- Appleby, A.J., *J. Electrochem. Soc.*, 1970, vol. 117, p. 328.
- Murthi, V.S., Urian, R.C., and Mukerjee, S., *J. Phys. Chem. B*, 2004, vol. 108, p. 11011.
- Wakabayashi, N., Takeichi, M., Uchida, H., and Watanabe, M., *J. Phys. Chem. B*, 2005, vol. 109, p. 5836.
- Chirkov, Yu.G. and Rostokin, V.I., *Elektrokhimiya*, 2006, vol. 42, p. 806 [*Russ. J. Electrochem. (Engl. Transl.)*, vol. 42, p. 722].
- Mitsushima, S., Araki, N., Kamiya, N., and Ota, K., *J. Electrochem. Soc.*, 2002, vol. 149, p. A1371.
- Parthasarathy, A., Srinivasan, S., Appleby, A.J., and Martin, C.R., *J. Electrochem. Soc.*, 1992, vol. 139, p. 2530.
- Ralph, T.R., Hards, G.A., Keating, J.E., Campbell, S.A., Wilkinson, D.P., Davis, M., St-Pierre, J., and Johnson, M.C., *J. Electrochem. Soc.*, 1997, vol. 144, p. 3845.
- Kocha, S.S, in *Handbook of Fuel Cells - Fundamentals, Technology and Applications*, Vielstich, W., Lamm, A., and Gasteiger, H., Eds., Chichester (UK): Wiley, 2003, vol. 3, ch. 43, p. 538.
- Gasteiger, H, Gu, W, Makharia, R, Mathias, M.F, and Sompalli, B, in *Handbook of Fuel Cells - Fundamentals, Technology and Applications*, Vielstich, W., Lamm, A., and Gasteiger, H., Eds., Chichester (UK): Wiley, 2003, vol. 3, ch. 46, p. 593.
- Gode, P., Lindbergh, G., and Sundholm, G., *J. Electroanal. Chem.*, 2002, vol. 518, p. 115.